PHYSICAL REVIEW E **77**, 041507 (2008)

Shear banding and yield stress in soft glassy materials

P. C. F. Møller,[1] S. Rodts,[2] M. A. J. Michels,[3] and Daniel Bonn[1,4]
[1]*Laboratoire de Physique Statistique, École Normale Supérieure, Paris, F-75231 France*
[2]*Navier Institute, University of Eastern Paris, Paris, F-77420 France*
[3]*Group Polymer Physics, Eindhoven University of Technology, Eindhoven, The Netherlands*
[4]*The van der Waals–Zeeman Institute, 1018 XE Amsterdam, The Netherlands*

(Received 10 July 2007; published 23 April 2008)

Shear localization is a generic feature of flows in yield stress fluids and soft glassy materials but is incompletely understood. In the classical picture of yield stress fluids, shear banding happens because of a stress heterogeneity. Using recent developments in magnetic resonance imaging velocimetry, we show here for a colloidal gel that even in a homogeneous stress situation shear banding occurs, and that the width of the flowing band is uniquely determined by the macroscopically imposed shear rate rather than the stress. We present a simple physical model for flow of the gel showing that shear banding (localization) is a flow instability that is intrinsic to the material, and confirm the model predictions for our system using rheology and light scattering.

DOI: 10.1103/PhysRevE.77.041507 PACS number(s): 83.50.-v, 83.60.Wc, 83.60.La, 83.60.Pq

If one stirs mayonnaise, sugar, or whipped cream with a spoon, it is easily observed that only a small fraction of the material closest to the spoon will be set in motion, the rest remaining "solid." This is a generic feature not only of traditional yield stress fluids such as mayonnaise [1] but also of glassy materials; recent simulations have shown for instance that the archetypical Lennard-Jones glass also shows localization of shear or "shear banding" [2].

Recently the analogy between yield stress and glassy materials has received much attention [1–4], and it has been realized not only that glasses have some features of yield stress materials but that the inverse is also true; for instance, *aging* and *shear rejuvenation* [5] are concepts that come from glasses, but their importance for determining the mechanical properties of yield stress fluids is by now well established [3–7]. Because this powerful analogy allowed improvement in our understanding of the mechanical properties of both glassy and yield stress materials, they are now called "soft glassy materials." The flow behavior of such soft glassy materials has been studied extensively: both colloidal [4,5,8–10] and polymer gels [11], emulsions [12], granular materials [13], colloidal glasses [4,14], pastes [15], and two-dimensional (2D) bubble rafts [16,17].

The most striking and general feature common to all of these systems is the observation of shear banding where the globally imposed shear rate is not distributed homogeneously, but localizes in highly sheared bands, while the remaining part of the fluid is not sheared at all [1,12,15]. In the classical picture of yield stress fluids, the material does not move if it is subjected to a stress smaller than the yield stress, and flows with a finite viscosity for a larger stress. In this case, shear banding is easy to understand as the consequence of a stress heterogeneity: the stress is above the yield stress where the material flows, and below it in the rest of the fluid [18]. However, it has been realized recently that in reality the generic flow curves of soft glassy materials differ from the simple yield stress fluid picture, and that notably very different results are obtained under an imposed shear rate and imposed stress [1,7,15]. This challenges also the "yield stress" view of shear banding.

In this paper we demonstrate that even in a homogeneous stress situation shear banding occurs, and that the width of the flowing band can be directly related to the macroscopically imposed shear rate. We present a simple physical model for a gel under shear flow that suggests that shear banding is a mechanical flow instability that is intrinsic to the material and is caused by an underlying flow curve with a negative slope. We confirm the negative slope by rheometry and the other predictions of the model by magnetic resonance imaging (MRI) velocimetry, rheology and light scattering.

The fluid used for the experiments is a gel formed from an aqueous suspension of charged colloidal particles (Ludox TM-40, Aldrich) in water. If a sufficient amount of salt (NaCl) is added to the solution, the Debye length, which gives the range of the electrostatic repulsions, decreases sufficiently for the van der Waals attraction between spheres to make them stick together. This leads to the formation of fractal, system-spanning networks of particles—a hard physical gel is formed [19]. The fluid is prepared by mixing a stock suspension of Ludox spheres with a 0.1 mass fraction salt water (NaCl) solution in the mass ratio 6:13 (giving a colloid volume fraction of 0.07), after which the fluid is left to age for at least 12 h. After this preparation the fluid gives reproducible results over periods of more than a week. More importantly, at an imposed shear rate the fluid reaches a steady state within minutes that is subsequently stable for hours [20]. Effectively this means that shearing the fluid for a few minutes "erases" the shear history of it prior to that shear, which is very important for practical experiments.

To examine if indeed shear banding can occur even when the stress is homogeneous, the fluid was loaded in a 4° cone-plate geometry with a 6 cm radius in a magnetic resonance imaging facility. Full description of the MRI setup can be found in [21]. For the purpose of our study, special MRI methods, developed to improve measurements of the velocity field inside Couette cells, were modified to suit a cone-plate geometry. As compared to standard MRI methodology [22], it allowed an increase in the usual signal to noise ratio of the experiment by up to two orders of magnitude, and made it possible to get complete 2D maps of the velocity

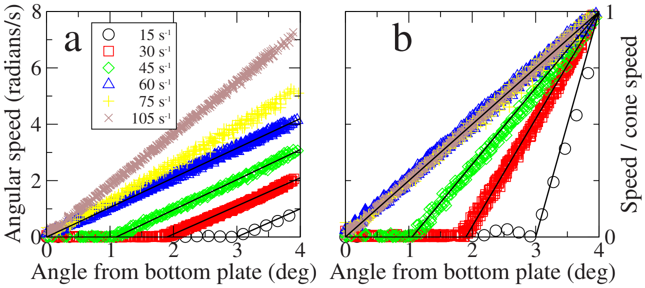

FIG. 1. (Color online) Velocity profiles in a 4° cone-plate geometry for different globally imposed shear rates. Fluid velocity (a) in rad/s and (b) normalized by the cone velocity.

field through an axial plane of the cell with a 0.125 mm axial and 1.2 mm radial space resolution, and with ±40 μm/s typical standard deviation on velocity values. For each MRI measurement, a new sample is loaded into the cell and presheared at 150 s^{-1} for 5 min to have a controlled shear history of the sample. Subsequently, the globally imposed shear rate is lowered to the one chosen for the experiment and the sample is allowed 5 min to reach a steady state before the MRI measurement is begun. Results for several imposed shear rates are shown in Fig. 1. At 60 s^{-1} and above, no shear banding is observed. Below 60 s^{-1} the shear rate is not homogeneous but zero in some parts and high in others, and while the fraction of the fluid that is sheared increases with $\dot{\gamma}_{\text{global}}$, $\dot{\gamma}_{\text{local}}$ in the flowing region is constant. Clearly, quite distinct shear banding occurs even in a homogeneous stress field. That the shear banding is uniquely determined by the macroscopically imposed shear rate is shown in Fig. 2(a), where the fraction of sheared material is given by a simple lever rule: In the sheared region $\dot{\gamma}_{\text{local}}=\dot{\gamma}_{\text{critical}}$, and the fraction sheared is given by $f=\dot{\gamma}_{\text{global}}/\dot{\gamma}_{\text{critical}}$ [7]. The critical shear rate can be extracted from Fig. 2(a) using both methods and they both give $\dot{\gamma}_{\text{critical}}=60\pm 1$ s^{-1}. Another important observation is that the transition between the sheared and the unsheared regions is very abrupt and the shear rate in the sheared region is constant in space, which is incompatible with a simple yield stress fluid behavior.

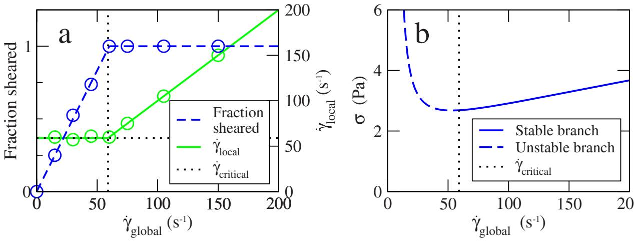

FIG. 2. (Color online) (a) The lever rule giving the fraction of the fluid that is sheared and the shear rate in that fraction depending on the critical shear rate. The data points are extracted from the fits in Fig. 1. (b) Steady state flow curve as given by the model. The branch to the right of the critical shear rate is stable while the branch to the left is unstable.

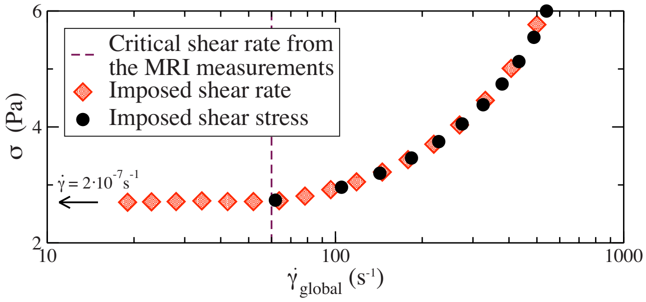

FIG. 3. (Color online) Steady state flow curves at imposed shear rate and shear stress. As predicted by the model the experiments coincide above the critical shear rate while they differ below—showing a stress plateau and no flow, respectively. For imposed shear rates below 20 s^{-1}, the recorded stress value is not stable but fluctuates, showing stick-slip behavior. This may be an indicator that the width of the sheared band becomes as small as the steady state cluster size in the band, leading to jamming. Note that here and elsewhere the microscopic model is applied only to the liquid phase, i.e., in steady state only above $\dot{\gamma}_c$—also in the shear banding regime. The arrow to the left indicates that for a stress 1% lower than the critical stress the resulting shear rate is 2×10^{-7} s^{-1}, which is solid to the resolution of our rheometer.

For micellar systems somewhat similar shear banding is observed and well understood as a coexistence of two phases in steady state coexistence—with viscosities differing by one to two orders of magnitude [23,24]. Our system is distinctly different in at least three aspects: (i) it is not in a steady state at low and zero shear rates where it is aging; (ii) it has a stress plateau between a low-viscosity branch and an infinite-viscosity branch, that is, it has a yield stress; and (iii) micellar systems are nonthixotropic in the sense that, given an imposed shear stress (except the plateau stress), they end up in the same final state independent of the initial state, but our system is very strongly thixotropic in the sense that a given imposed stress can result in completely different behavior depending on the initial state of the fluid. Point (i) is demonstrated in Fig. 5, point (ii) in Fig. 3, and point (iii) in Fig. 4. Hence the models for micellar fluids do not apply to our system, which needs a new theoretical understanding, to be provided below.

Although not exactly zero, the relative stress variation in a 4° cone-plate geometry is less than 0.005 and effectively negligible (as shown by the constant shear rate in the sheared band). In addition, results with an 8° cone-plate device (having a stress heterogeneity four times as large) yielded similar results, showing that the shear banding is not due to stress heterogeneities. To understand shear banding in a homogeneous stress field, we develop a simple model to take into account the interplay between viscosity, flow, and the colloidal microstructure in the fluid. To qualitatively capture the observed thixotropic behavior of the gel, we assume the following.

(i) In time the colloidal particles aggregate into fractal clusters that are nondraining [25]; $\phi=\phi(t)$ is then the "hydrodynamic" volume fraction determined by the aggregate radius $R(t)$, rather than the much smaller actual volume fraction ϕ_0 of particles with radius R_0. The number of fractal aggregates decreases in inverse proportion to the aggregate mass $M\sim R^{d_f}$, while their hydrodynamic volume scales as R^3, so $\phi(t)/\phi_0=[R(t)/R_0]^{3-d_f}$. Since $d_f<3$ it is clear that continued aggregation will lead with time to a percolating gel.

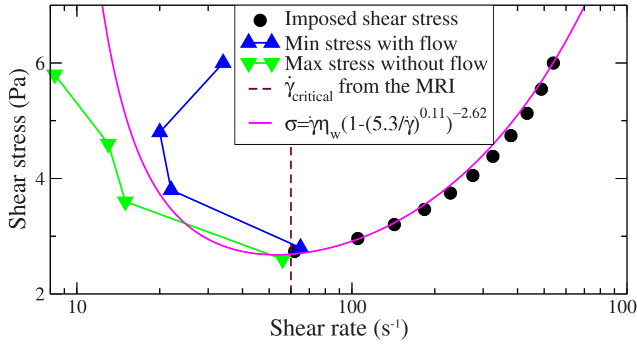

FIG. 4. (Color online) Full steady state flow curve found using two different types of measurements. The stable branch is simply found from imposing the shear stress, while the unstable branch can be pinned from the left and right by (for each of several material ages) finding initial σ-$\dot{\gamma}$ points that respectively slow down and speed up under imposed shear stress. From the lower right corner the aging time after preshear at 150 s^{-1} is 0, 10, 500, and 3000 s. The model is also seen to provide an excellent fit to the data. The fitted parameters $n(3-d_f)=0.11$ and $s=2.62$ are of the right order of magnitude; the value for $n(3-d_f)$ is slightly lower than expected, but not inconsistent with a fractal dimension well above that of, e.g., DLCA, due to compaction under shear.

(ii) The effective viscosity η depends on the hydrodynamic volume fraction ϕ of the dispersed particles via a Krieger-Dougherty [26], mean-field [27,28], or more general scaling-type expression $\eta/\eta_0=(1-\phi/\phi_p)^{-s}$, with η_0 the solvent viscosity and ϕ_p a gel-percolation point well below unity; the exponent s will be 2, $2.5\phi_p$ [26], 1 [27], or left as a fitting parameter, dependent on the chosen expression, but will anyway be of order unity.

(iii) The flow breaks up the aggregates. Via different mechanistic assumptions of aggregation and breakup, different models can be constructed for the rate of change dM/dt of the cluster mass. Depending on the stress or strain rate applied, a steady state $dM/dt=0$ may or may not be reached between spontaneous aggregation and flow-induced breakup, which relates R to $\dot{\gamma}$. Fairly independently of the specific model, e.g., diffusion-limited cluster aggregation (DLCA, $d_f=1.7-1.8$) [29] or shear-induced aggregation [30], size scaling in fracture, etc., one arrives at a relation of the form $R/R_0=(\dot{\gamma}/\dot{\gamma}_0)^{-n}$, with $\dot{\gamma}_0$ some typical high shear rate and n a model-dependent exponent smaller than unity; e.g., DLCA with breakup linearly proportional to the shear rate may be shown to give $n=1/d_f=0.55-0.60$, while for shear-induced aggregation a value $n=1/3$ has been derived, in good agreement with some experimental data [30]. Rheometric studies with a similar modeling approach also show that shear may lead to more compact aggregates, with an increase in d_f toward 2.4–2.5 [31].

Combination of (i), (ii), and (iii) gives an effective steady state shear stress that depends on shear rate:

$$\sigma_{ss}(\dot{\gamma}) = \dot{\gamma}\eta_0\left[1-\left(\frac{\dot{\gamma}_p}{\dot{\gamma}}\right)^{(3-d_f)n}\right]^{-s} \qquad (1)$$

with $\dot{\gamma}_p$ corresponding to the percolation point ϕ_p also via (i)–(iii): $\dot{\gamma}_p=\dot{\gamma}_0(\phi_0/\phi_p)^{1/(3-d_f)n}$. The resulting *steady state flow curve* σ_{ss} vs $\dot{\gamma}$ is shown in Fig. 2(b).

The most important feature of the model is that it gives rise to a critical shear rate $\dot{\gamma}_c=\dot{\gamma}_p[1+sn(3-d_f)]^{1/(3-d_f)n}$ for which the slope of stress vs strain rate changes sign [3]. The negative slope for $\dot{\gamma}<\dot{\gamma}_c$ implies that such flows are unstable [32] which, as will follow, is the hallmark of shear banding.

Cohen and co-workers recently examined colloidal crystal subjected to oscillatory shear [14]. They observed that the colloids shear band into a hcp crystal and a state where crystal layers slide over each other. These two states can in fact be understood as limiting cases of ours; those of infinite and unit cluster sizes, respectively. This is consistent with the finding of Cohen and co-workers that their system shows a transition between two linearly responding phases—one solid and one liquid.

We will now test the detailed predictions of the model using standard rheology. The rheology was done also with a 4° cone-plate cell but now of 2 cm radius in a Rheologica Stresstech rheometer. The essence of the model is the competition between spontaneous buildup of the colloidal aggregates, increasing the viscosity, and breakdown by the flow, decreasing it. Thus, either the viscosity becomes infinite, or it decreases due to the flow to a steady state and rather low value. If the shear rate is imposed, this can lead to shear banding (the viscosity being infinite in one part and low in the other), but if the stress is imposed the whole material is either solid *or* fluid [7]. This is known as viscosity bifurcation [6]. The model then predicts that measurements at imposed shear stress and imposed shear rate should coincide when $\dot{\gamma}_{\text{global}}$ is above $\dot{\gamma}_{\text{critical}}$ and differ below it; while the measurements at imposed stress should give an infinite viscosity, the steady state measurements at imposed shear rate should give rise to a stress plateau according to the lever rule. Using imposed shear rate and imposed stress experiments, excellent qualitative agreement with the model predictions and quantitative agreement with the critical shear rate found from the MRI measurements is obtained (Fig. 3).

To obtain the negative slope of the flow curve, we note that all points in Fig. 2(b) can be visited, if only temporarily. In general, a point above the steady state flow curve of Fig. 2(b) is a fluid subject to a stress that is too high for its cluster size to be stable, so it decreases in time and leads to a lower viscosity. Under an imposed shear stress the resulting shear rate increases in time and the flow point moves to the right. Conversely, if one starts out at a point below the steady state flow curve the point moves to the left. The flow curve (in particular the unstable part of it) can then be obtained by looking at the transition between points that move to the right and to the left, as is done in Fig. 4, where it is evident that indeed the flow curve has a negative slope below the critical shear rate. In addition to qualitative agreement between our model and data a quantitative fit of the full flow curve can be made using Eq. (1), which describes the data very well.

Perhaps the strongest prediction of the model is that, if shear banding is observed, the state of the fluid in the flowing part should be significantly different from that in the quiescent part. This contradicts the classical yield stress picture, which claims that shear banding is due to stress inhomogeneities and not to "age" inhomogeneities in an otherwise identical material under homogeneous stress. To test this prediction, we measured the structural relaxation time of the fluid in the solid and in the sheared band using diffusing wave spectroscopy (DWS); By measuring the time correlation of laser light diffusing through the fluid, one gains information about the motion of the individual scatterers in the fluid and hence its structural relaxation time and viscosity [33]. To do such a measurement we constructed a Couette cell (inner and outer radii of 75 and 95 mm) with a laser parallel to the rotation axis to perform DWS measurements of the fluid at different positions within the gap. For each gap position the flow was briefly stopped for the duration of the DWS measurement. The DWS measurements give a wealth of information that can be read off from Fig. 5 directly [4]: Longer correlation times correspond to longer structural relaxation times of the fluid and hence higher viscosities. For a material in a liquid, ergodic state the correlation function decays rapidly—as do the measurements in the sheared band. Correlation functions that do not decay to zero, such as those in the nonsheared band, demonstrate that the material is in a nonergodic out-of-equilibrium state that is aging—just like glasses. Very interestingly almost identical findings were reported in a numerical study of the classic Lennard-Jones glass [2]. The fact that aging effects are demonstrated to be crucial for understanding shear banding in both a simple numerical and an actual experimental system hints that the concept of a steady state flow curve with a negative slope may be key to understanding shear banding in many, if not all, aging systems.

In sum, all of our observations agree with the hypothesis that shear banding is not due to a stress heterogeneity, but is intrinsic to the fluid. Using MRI velocimetry we demonstrated that shear banding can occur even in homogeneous stress fields and that the width of the sheared band is simply given by a lever rule: knowing the critical shear rate (for instance from macroscopic rheology experiments), shear banding can be predicted. A simple physical model can account for shear banding as an intrinsic property of the fluid, from which the critical shear rate follows naturally. This is likely to be general for soft glassy materials; it relies on the viscosity bifurcation, which has been observed for a wide variety of systems: colloidal glasses and gels, granular matter, foams and emulsions, and polymer gels, all of which also exhibit shear banding.

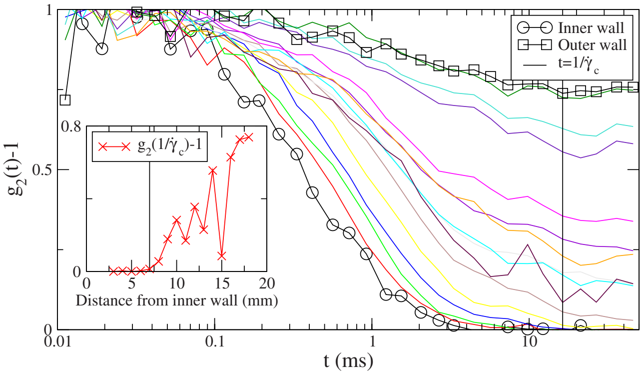

FIG. 5. (Color online) DWS time correlation measurements of the fluid inside and outside the sheared band in a Couette geometry. The inset shows the correlation function at $t=1/\dot{\gamma}_c$ (which is a characteristic relaxation time of the material) as function of the distance from the inner wall. The tendency for much longer correlation times in the solid phase as compared to the sheared phase is very clear, and similar to a simulation of a model glass that exhibits shear banding [2].

---

[1] P. Coussot, J. S. Raynaud, F. Bertrand, P. Moucheront, J. P. Guilbaud, H. T. Huynh, S. Jarny, and D. Lesueur, Phys. Rev. Lett. **88**, 218301 (2002).
[2] F. Varnik, L. Bocquet, J. L. Barrat, and L. Berthier, Phys. Rev. Lett. **90**, 095702 (2003).
[3] P. Coussot, Q. D. Nguyen, H. T. Huynh, and D. Bonn, Phys. Rev. Lett. **88**, 175501 (2002).
[4] D. Bonn, S. Tanase, B. Abou, H. Tanaka, and J. Meunier, Phys. Rev. Lett. **89**, 015701 (2002).
[5] F. Ianni, R. Di Leonardo, S. Gentilini, and G. Ruocco, Phys. Rev. E **75**, 011408 (2007).
[6] P. Coussot *et al.*, J. Rheol. **46**, 573 (2002).
[7] P. Møller *et al.*, Soft Matter **2**, 274 (2006).
[8] S. Manley *et al.*, Phys. Rev. Lett. **93**, 108302 (2004).
[9] L. Cipelletti, S. Manley, R. C. Ball, and D. A. Weitz, Phys. Rev. Lett. **84**, 2275 (2000).
[10] A. Dinsmore, V. Prasad, I. Y. Wong, and D. A. Weitz, Phys. Rev. Lett. **96**, 185502 (2006).
[11] F. K. Oppong, L. Rubatat, B. J. Frisken, A. E. Bailey, and J. P. de Bruyn, Phys. Rev. E **73**, 041405 (2006).
[12] L. Becu, S. Manneville, and A. Colin, Phys. Rev. Lett. **96**, 138302 (2006).
[13] F. da Cruz, S. Emam, M. Prochnow, J. N. Roux, and F. Cehoir, Phys. Rev. E **72**, 021309 (2005).
[14] I. Cohen, B. Davidovitch, A. B. Schofield, M. P. Brenner, and D. A. Weitz, Phys. Rev. Lett. **97**, 215502 (2006).
[15] N. Huang, G. Ovarlez, F. Bertrand, S. Rodts, P. Coussot, and D. Bonn, Phys. Rev. Lett. **94**, 028301 (2005).
[16] J. Lauridsen, G. Chanan, and M. Dennin, Phys. Rev. Lett. **93**, 018303 (2004).
[17] C. Gilbreth, S. Sullivan, and M. Dennin, Phys. Rev. E **74**, 051406 (2006).
[18] H. Zhu *et al.*, J. Non-Newtonian Fluid Mech. **129**, 177 (2005).
[19] R. G. Larson, *The Structure and Rheology of Complex Fluids* (Oxford University Press, Oxford, 1999).
[20] In order to achieve this it was found necessary to gently shear the fluid for 1 min just after mixing.
[21] J.-S. Raynaud *et al.*, J. Rheol. **46**, 709 (2002).
[22] S. Stapf and S. L. Han, *NMR Imaging in Chemical Engineering* (Wiley-VCH, Weinheim, 2006).
[23] S. Manneville, A. Colin, G. Waton, and F. Schosseler, Phys. Rev. E **75**, 061502 (2007).
[24] M. López-González, W. M. Holmes, P. T. Callaghan, and P. J. Photinos, Phys. Rev. Lett. **93**, 268302 (2004).

[25] P. Wiltzius, Phys. Rev. Lett. **58**, 710 (1987).
[26] I. M. Krieger, Adv. Colloid Interface Sci. **3**, 111 (1972).
[27] N. Saito, J. Phys. Soc. Jpn. **5**, 4 (1950); **7**, 447 (1952).
[28] D. Bedeaux, J. Colloid Interface Sci. **118**, 80 (1987).
[29] D. A. Weitz, J. S. Huang, M. Y. Lin, and J. Sung, Phys. Rev. Lett. **53**, 1657 (1984).
[30] R. Wessel and R. C. Ball, Phys. Rev. A **46**, R3008 (1992).
[31] W. Wolthers *et al.*, J. Rheol. **40**, 799 (1996).
[32] R. I. Tanner, *Engineering Rheology* (Clarendon, Oxford, 1985).
[33] D. J. Pine, D. A. Weitz, P. M. Chaikin, and E. Herbolzheimer, Phys. Rev. Lett. **60**, 1134 (1988).